The American Journal of Pathology, Vol. 172, No. 5, May 2008

DOI: 10.2353/ajpath.2008.070730

Metabolic, Endocrine and Genitourinary Pathobiology

Retinal Dysfunction and Progressive Retinal Cell Death in SOD1-Deficient Mice

Kouhei Hashizume,*† Manabu Hirasawa,* Yutaka Imamura,* Setsuko Noda,‡ Takahiko Shimizu,§ Kei Shinoda,¶‖ Toshihide Kurihara,* Kousuke Noda,* Yoko Ozawa,* Susumu Ishida,* Yozo Miyake,¶ Takuji Shirasawa,§ and Kazuo Tsubota*

From the Department of Ophthalmology, Inaida Laboratory, Keio University School of Medicine, Tokyo; the Department of Ophthalmology,† Iwate Medical University School of Medicine, Morioka; the Department of Health Science,‡ Tokai University School of Nursing, Kanagawa; the Research Team for Molecular Biomarkers,§ Tokyo Metropolitan Institute of Gerontology, Tokyo; the Department of Ophthalmology,¶ National Institute of Sensory Organs, Tokyo Medical Center, Tokyo; and the Department of Ophthalmology,‖ Oita University School of Medicine, Oita, Japan*

The superoxide dismutase (SOD) family is a major antioxidant system, and deficiency of Cu,Zn-superoxide dismutase (SOD1) in mice leads to many different phenotypes that resemble accelerated aging. The purpose of this study was to examine the morphology and physiology of the sensory retina in *Sod1*$^{-/-}$ mice. The amplitudes of the a- and b-waves of electroretinograms elicited by stimuli of different intensity were reduced in senescent *Sod1*$^{-/-}$ mice, and this reduction in amplitude was more pronounced with increasing age. Retinal morphometric analyses showed a reduced number of nuclei in both the inner nuclear cell layer and outer nuclear cell layer. Electron microscopy revealed swollen cells and degenerated mitochondria in the inner nuclear cell and outer nuclear cell layer of senescent *Sod1*$^{-/-}$ mice indicating necrotic cell death. Terminal deoxynucleotidyl transferase-mediated dUTP nick end labeling revealed no significant differences in the number of apoptotic cells between *Sod1*$^{-/-}$ and wild-type mice, and activated caspase-3 could not be detected in the retina of *Sod1*$^{-/-}$ mice. In addition to the age-related macular degeneration-like phenotypes previously reported, *Sod1*$^{-/-}$ mice also present progressive retinal degeneration. Our results indicate that *Sod1*$^{-/-}$ mice may be a good model system in which to study the mechanism of reactive oxygen species-mediated retinal degeneration. *(Am J Pathol 2008, 172:1325–1331; DOI: 10.2353/ajpath.2008.070730)*

The superoxide dismutase (SOD) family is one of the main antioxidant systems in the body and is made up of the three SOD isoenzymes; Cu,Zn-superoxide dismutase (SOD1) exists in the cytoplasm, SOD2 or Mn-SOD in the mitochondrial matrix, and SOD3 or extracellular SOD in the interstitium of tissues as the secreted form.[1] SOD1 catalyzes superoxide radical dismutation and is distributed throughout the body,[1] and among the three isozymes, it is the most abundant in the retina.[2] This suggests that SOD1 may be important in protecting the sensory retina from the reactive oxygen species (ROS)-mediated retinal damage.

Many models of retinal degeneration have been studied[3,4]; however, the mechanism of retinal cell deaths in some of these models has still not been determined. Cell death can be either necrotic or apoptotic, and necrotic cell death is characterized by a swelling of the cell membranes and organelles that leads to a disruption of the cell membranes and lysis. These alterations subsequently lead to inflammatory responses.[5] Apoptosis is a process of programmed cell death, and involves an orchestrated series of biochemical events leading to characteristic cell morphology and death. In some models of retinal degeneration, the death of the neurons has been shown to be attributable to apoptosis.[6–8]

SOD1 deficiency (*Sod1*$^{-/-}$) leads to many different phenotypes resembling aging, and the changes are attributable to an elevation of ROS.[9,10] We recently reported that senescent *Sod1*$^{-/-}$ mice had features of age-related macular degeneration (AMD) including the presence of drusen, choroidal neovascularization, and retinal pigment epithelium dysfunction.[11] Because SOD1 is expressed throughout the retina and not only in the retinal pigment epithelium,[11] we have hypothesized that the SOD1 deficiency will alter the morphology and physiology of the retina of *Sod1*$^{-/-}$ mice. To examine this hypothesis, we investigated the morphology of the retina of *Sod1*$^{-/-}$ mice of different ages by morphometric meth-

Accepted for publication January 24, 2008.

K.H. and M.H. contributed equally to this study.

Present address of T.S.: Department of Aging Control Medicine, Juntendo University Graduate School of Medicine, Tokyo, Japan.

Address reprint requests to Yutaka Imamura, M.D., Department of Ophthalmology, Inaida Laboratory, Keio University School of Medicine, 35-Shinanomachi, Shinjuku-ku, Tokyo 160-8582, Japan. E-mail: imamura@sc.itc.keio.ac.jp.

ods and the retinal function by electroretinography. We shall show that the amplitudes of the electroretinograms (ERGs) elicited by different light stimuli were reduced in senescent *Sod1*$^{-/-}$ mice. Morphometric analyses of the retina of *Sod1*$^{-/-}$ mice of different ages showed evidence of necrotic cell death in the retinal cell layers.

Materials and Methods

Animals

Sod1$^{-/-}$ mice that were backcrossed to C57BL/6 and wild-type (WT) mice were studied.[11] All animal experiments were performed in accordance with the Association for Research in Vision and Ophthalmology Statement for the Use of Animals in Ophthalmic and Vision Research.

ERGs

ERGs were recorded as described in detail.[12–14] Briefly, animals were dark-adapted for at least 12 hours and prepared under dim red illumination. A contact lens electrode carrying light-emitting diodes (WLS-20; Mayo Corporation, Inazawa, Japan) was used for the recordings and stimulations. The ERGS were differentially amplified and filtered with the band pass filters set from 0.3 to 500 Hz for the a- and b-waves. White light pulses of 0.009, 3.0, and 65.0 cd*sm^{-2} were obtained from the light-emitting diodes embedded in the contact lens electrode. The stimulus duration was 0.03, 3.0, and 5.0 ms for 0.009, 3.0, and 65.0 cd*sm^{-2}, respectively. The interstimulus interval was 2 seconds for 0.009 cd*sm^{-2} and 15 seconds for the two higher intensities.

To isolate the cone pathway, mice were exposed to a white adapting field of 25 cd*m^{-2} for 10 minutes, and the photopic and flicker ERGs were elicited by white light pulses of 3 ms delivered at a frequency of 1 and 10 Hz. The stimuli were presented on the white adapting field. Five to fifteen responses were averaged for the single-flash ERGs, and 15 responses for the 10-Hz flicker ERGs. The amplitude of the a-wave was measured from baseline to the trough of the a-wave, and the b-wave was measured from the trough of the a-wave to the peak of the b-wave. The implicit time was measured from the onset of the stimulus to the peak of the a- or b-waves.

Retinal Morphometry and Electron Microscopy

The enucleated eyes were immediately embedded in optimal cutting temperature (OCT) compound (Lab-Tek Products, Naperville, IL) and frozen in dry ice-ethanol for cryosectioning. The sections were stained with hematoxylin and eosin. Horizontal sections were cut through the optic nerve, and sections were obtained from WT and *Sod1*$^{-/-}$ mice (KO) at 10, 30, and 50 weeks of age (n = 10, each group). Sections with at least 20 rows of inner nuclear cell layer (INL) and outer nuclear cell layer (ONL) were selected, and the number of nuclei/column was calculated as described with slight modifications.[15] The ratios of the number of nuclei in the *Sod1*$^{-/-}$ to WT (*Sod1*$^{-/-}$/WT) numbers were used for the statistical analyses. For transmission electron microscopy, tissues were fixed, prepared, and observed as previously reported.[11]

Terminal Deoxynucleotidyl Transferase-Mediated dUTP Nick End Labeling (TUNEL) Staining

TUNEL was performed to detect apoptosis in the retina with the *in situ* cell death detection kit, POD (Roche Molecular Biochemicals, Indianapolis, IN). Briefly, frozen sections were fixed in 4% paraformaldehyde in phosphate-buffered saline (PBS) and incubated in 0.1% Triton X-100 and 0.1% sodium citrate for 2 minutes at 4°C, rinsed twice in PBS, followed by incubation in 0.3% H_2O_2-containing methanol for 30 minutes at room temperature to block the endogenous POD activity. After washing in PBS, sections were incubated with the TUNEL reaction mixture containing terminal deoxynucleotidyl transferase in a moist chamber overnight at 4°C, washed again with PBS, and incubated with TUNEL POD for 1 hour at room temperature. To make the apoptotic cells visible, sections were incubated with 3′-diaminobenzidine as a chromogen and counter stained with hematoxylin.

Western Blots and Immunohistochemistry for Caspase

Western blot analysis for procaspase-3 and cleaved caspase-3 was performed with retina lysates. Briefly, retinas were sonicated in 0.5% Nonidet P-40, 10 mmol/L Tris-HCl (pH 7.5), and 150 mmol/L NaCl containing Complete Protease Inhibitor cocktail (Roche Diagnostics GmbH, Mannheim, Germany). Tissue homogenates were centrifuged at 15,000 × g for 30 minutes, and equal amounts (20 μg) of tissue extract were added to 15% sodium dodecyl sulfate-polyacrylamide gel electrophoresis and electroblotted onto an Immobilon-P membrane (Millipore, Bedford, MA). The membranes were blocked in 5% skim milk in Tris-buffered saline and probed with antibodies against caspase-3 (1:1000, 8G10; Cell Signaling, Danvers, MA). Immunoreactive procaspase-3 and cleaved caspase-3 were made visible with the ECL system (Amersham Biosciences, Piscataway, NJ) and luminoimage analyzer LAS-3000 (Fuji Film, Tokyo, Japan). For control, confluent NIH 3T3 cells were treated and incubated with 1 μmol/L staurosporine for 8 hours, and cell lysates were analyzed. Immunohistochemistry with anti-cleaved caspase-3 antibody (no. 9661, Cell Signaling) were performed for WT and KO with different ages (10 weeks, 30 weeks, and 50 weeks), following the manufacturer's protocol. Nuclei were counterstained with 4,6-diamidino-2-phenylindole. Sections were prepared from mammary tissues from 2-week-old mice after weaning to obtain positive controls.

Statistical Analyses

Data are presented as the means ± SE of the means (SEMs), and analyzed with Student's t-tests. For the thick-

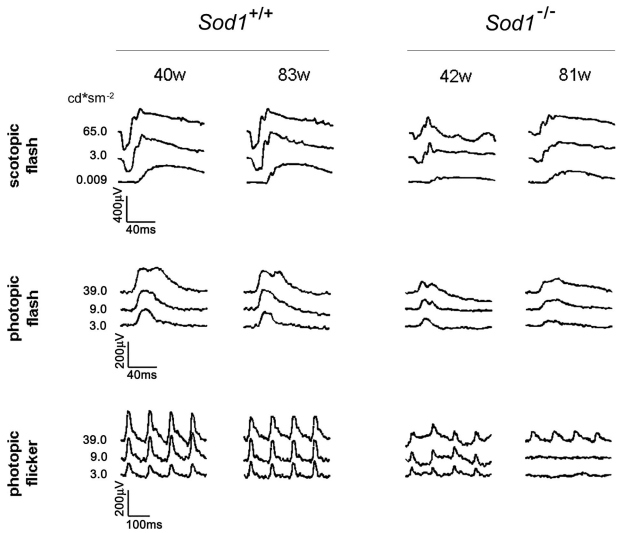

Figure 1. ERGs recorded from age-matched WT and *Sod1*$^{-/-}$ mice. Data of two representative cases of the WT and two *Sod1*$^{-/-}$ mice are shown. ERGs were recorded under three different stimulus conditions (scotopic flash, photopic flash, photopic flicker). Stimulus intensities are shown at the **left**.

ness of the ONL and INL, Kruskal-Wallis test followed by Bonferroni post hoc test was performed to evaluate differences at all periods. A P value <0.05 was considered statistically significant.

Results

ERGs

Representative scotopic, photopic, and 10-Hz flicker ERGs recorded from a 42-week-old mouse and an 81-week-old *Sod1*$^{-/-}$ mouse, and a 40-week-old mouse and an 83-week-old WT mouse are shown Figure 1. The ERGs were elicited by different stimulus intensities. At present, it is known that the scotopic a-wave originates from the activity of rods, and the scotopic and photopic b-waves from a depolarization of the on-bipolar cells and potassium efflux from the Mueller cells. The photopic ERGs and the 10-Hz flicker responses originate from the cones and cone-driven bipolar cells.

Our recordings showed that both the a- and b-waves were reduced at the age of 40 weeks. The reduction in the a- and b-waves in *Sod1*$^{-/-}$ mice was found at all stimulus intensities (Figure 2). The ages of the mice in each group were as follows [mean ± SE (range)]: 59.1 ± 7.6 (39.9 to 82.6) weeks in WT, and 57.9 ± 6.4 (42.4 to 80. 5) weeks in KO. At younger ages, ie, <20 weeks, the amplitudes of the ERGs in the two groups were not significantly different. However, the amplitudes of the scotopic a-waves (Figure 3A) and b-waves (Figure 3B) gradually decreased with increasing age in the *Sod1*$^{-/-}$ mice. Therefore, senescent *Sod1*$^{-/-}$ mice exhibited functional disturbances of both the outer and inner sensory retina. It is interesting that the oscillatory potentials were preserved even in a very old *Sod1*$^{-/-}$ mouse showing decreased amplitudes of a- and b-waves (Figure 1).

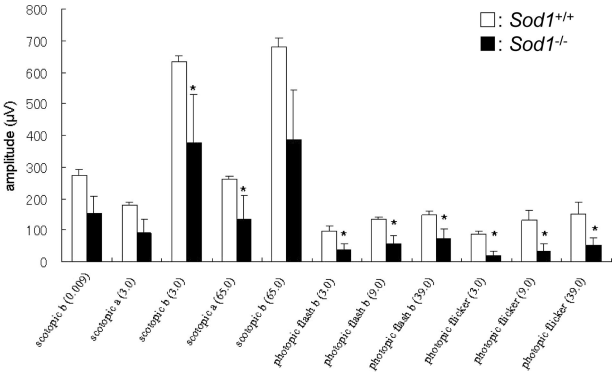

Figure 2. Mean amplitudes of a- and b-waves of the ERGs. ERGs were recorded from age-matched WT and *Sod1*$^{-/-}$ mice >40 weeks of age (n = 5, each group). **Asterisk** indicates $P < 0.05$. **White box**, WT; **black box**, *Sod1*$^{-/-}$.

Retinal Histology and Ultrastructure

The thicknesses of the retinal layers of WT and the *Sod1*$^{-/-}$ mice at 10, 30, and 50 weeks of age were measured. The differences in the thicknesses of the INL and ONL were not significant for the two types of mice up to the age of ~10 weeks. Thereafter, the thickness of the ONL and INL in *Sod1*$^{-/-}$ mice gradually decreased (Figure 4). The ratios (KO/WT) of the numbers of nuclei per row were 100.4%, 97.9%, and 81.4% in the INL, and 93.6%, 85.2%, and 71.9% in the ONL at ages 10, 30, and 50 weeks, respectively. The significant decrease in the thickness started at 50 weeks in the INL ($P < 0.01$) and 30 weeks in the ONL ($P < 0.05$), indicating that the photoreceptors, horizontal, bipolar, amacrine, and Mueller cells were most likely damaged in the senescent *Sod1*$^{-/-}$ mice.

Ultrastructural examination showed a disorganized INL and ONL in 15-month-old senescent *Sod1*$^{-/-}$ mice (Figure 5, A–F). The nuclei were swollen, the cytoplasm was vacuolized, and the plasma and nuclear membranes in the INL were disrupted in a *Sod1*$^{-/-}$ mouse at 15 months of age (Figure 5, A and B). The ONL was also disorganized in contrast to the orderly alignment of each column of nuclei in the WT, and the density also decreased in the *Sod1*$^{-/-}$ mice (Figure 5, C and D). The mitochondria in the ONL were damaged, and the cell bodies were swollen. Necrotic cells were also observed (Figure 5F). We rarely observed retinal cells showing chromatin condensation, a morphological hallmark of apoptotic cell. These findings suggest that the death of the neurons in *Sod1*$^{-/-}$ mice was attributable to necrosis possibly because of elevated ROS.

Cell Deaths in Retinas of Senescent *Sod1*$^{-/-}$ Mice Is Not Caspase-3-Dependent

To explore the mechanism of cell death, we first examined if the apoptotic pathways were activated in retinas of *Sod1*$^{-/-}$ mice at ages 30 and 50 weeks. TUNEL staining showed that the difference between the WT and *Sod1*$^{-/-}$ mice was not significant (data not shown). Next, we performed Western blot analysis for the detection of the

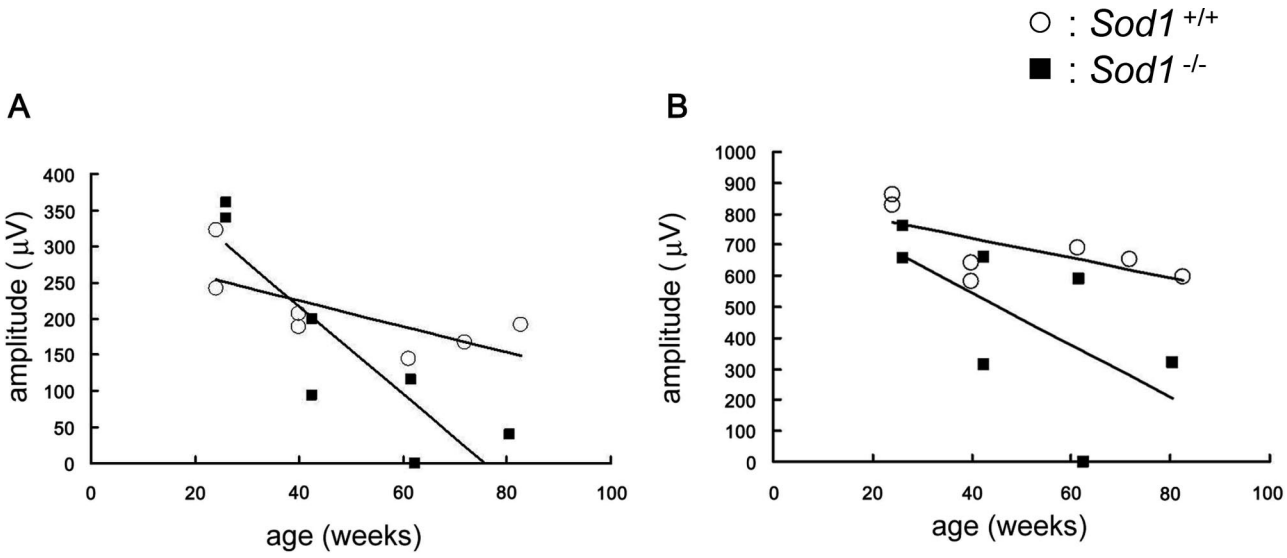

Figure 3. Age-related changes of ERGs. **A:** Age-related changes of the amplitudes of the scotopic a-wave. The amplitudes decrease with increasing age in *Sod1*$^{-/-}$ mice (**black squares**), in contrast to those of the WT (**white circles**). **B:** Age-related changes of the scotopic b-wave. Stimulus intensity was 65.0 cd*sm^{-2}.

active form of caspase, however the activated form of caspase-3 was not apparent in the *Sod1*$^{-/-}$ mice. Immunohistochemistry with anti-cleaved caspase-3 antibody did not show apparent positive signals in the sensory retinas of KO and WT mice as compared with a positive control (data not shown). Therefore, the retinal degeneration of *Sod1*$^{-/-}$ mice appears not to be dependent mainly on apoptosis as in some other models of retinal degeneration.[6–8] Considering that SOD1 is the most abundant antioxidant that scavenges superoxide in retina, cell deaths in ONL of *Sod1*$^{-/-}$ mice might be caused by the ROS-mediated necrotic pathway, rather than by the apoptotic pathways, as was compatible with the ultrastructural findings. Because the presence of inflammatory reactions is a hallmark of necrosis, diffuse deposition of immunoglobulins in retina-retinal pigment epithelium complex in *Sod1*$^{-/-}$ mice[11] might be attributable to necrotic reactions. However, we are aware of the possibility that very slow apoptotic cell deaths could contribute to the retinal dysfunction in these mice.

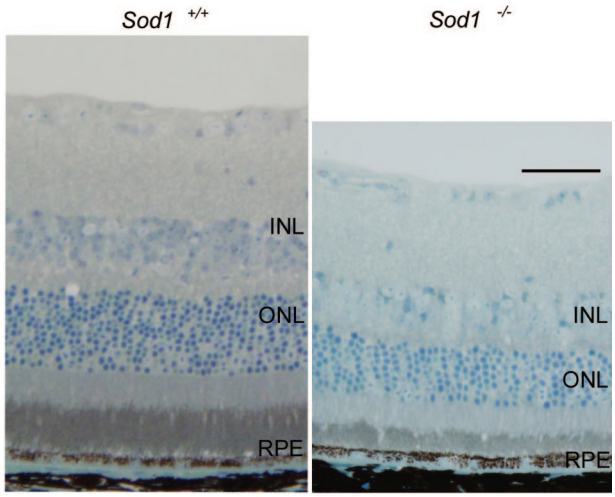

Figure 4. Retinal thinning of *Sod1*$^{-/-}$ mice. Toluidine blue-stained retina Quetol 812 sections (2 μm) of a 15-month-old WT mouse and an age-matched *Sod1*$^{-/-}$ mouse. Thinning of the INL and ONL is apparent. Scale bar = 50 μm.

Discussion

Our results showed that retina of SOD1-deficient mice had morphological and functional alterations that increased with increasing age. When mice were young (<5 months), the retinas appeared not significantly different from those of WT mice when examined by ophthalmoscopy.[11]

Different Roles of SOD1 and SOD2 in Retina

SOD1 and SOD2 are two major intracellular SODs and both are ubiquitously distributed in the sensory retina.[11] The retinas of *Sod2*$^{-/-}$ mice are thinner than the same age WT mice even at birth.[16] Because *Sod2*$^{-/-}$ mice die soon after birth by dilated cardiomyopathy,[17] *Sod2*$^{-/-}$ mice are not suitable for the examination of age-related retinal dysfunction attributable to accumulated ROS. Current technical modalities for conditional knockout of SOD2 would be expected to overcome this problem.[18] In contrast to the acute and severe retinal degeneration in *Sod2*$^{-/-}$ mice, the degeneration in *Sod1*$^{-/-}$ mice is mild and slowly progressive. Because the amounts of SOD2 and SOD3 proteins are approximately the same in WT and *Sod1*$^{-/-}$ mice,[11] other oxidative stress scavenger systems such as SOD2 may at least partially protect the retina against ROS-mediated retinal damages in *Sod1*$^{-/-}$ mice *in vivo*.

SOD1 Is Necessary to Prevent Age-Related Degeneration of Sensory Retina

In addition to the retinal changes, the *Sod1*$^{-/-}$ mice have a short lifespan,[9] ovarian dysfunction,[19] liver tumors,[9]

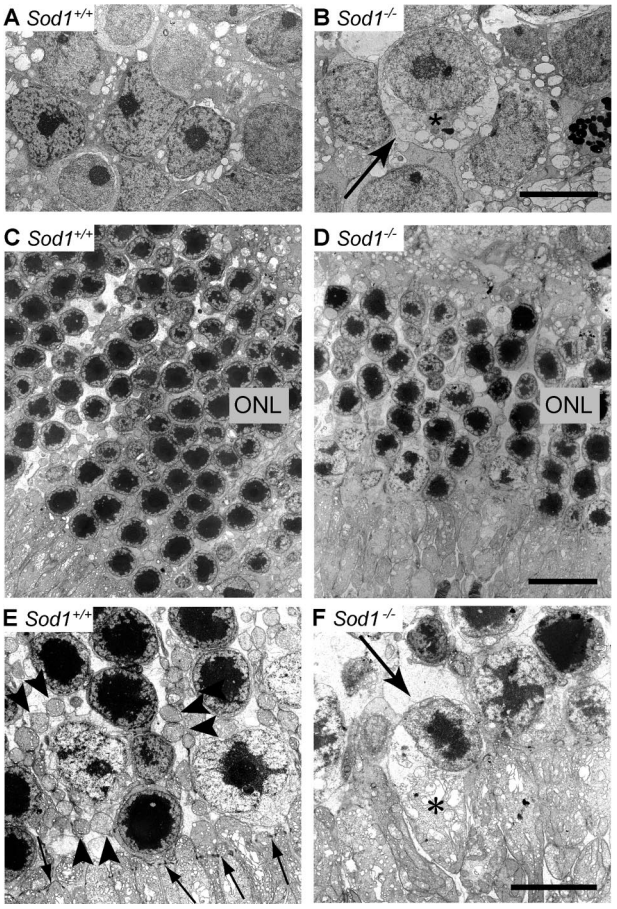

Figure 5. Ultrastructure of sensory retina of the senescent WT and age-matched *Sod1*$^{-/-}$ mice. **A:** INL of the WT of 15 months. **B:** Swollen nuclei in the INL of age-matched *Sod1*$^{-/-}$ mice (**asterisk**). Vacuolization and destruction of plasma and nuclear membranes can be seen (**arrow**). **C:** ONL of a WT mouse at 15 months of age. **D:** ONL of an age-matched *Sod1*$^{-/-}$ mouse. Cell layers are disorganized, and the cell density is decreased. The number of nuclei in the ONL is decreased in *Sod1*$^{-/-}$ mice. Higher magnification of ONL. WT (**E**), and *Sod1*$^{-/-}$ mice (**F**). Mitochondria in photoreceptors of ONL distinguished in *Sod1*$^{-/-}$ mice, as compared with the WT (**arrowheads** in **E**). External limiting membrane in the WT (**arrows** in **E**) is not distinct in a 15-month-old *Sod1*$^{-/-}$ mouse. Plasma membranes are not clear in a damaged cell of the *Sod1*$^{-/-}$ mouse (**arrow** in **F**). Swelling of the inner segments of the photoreceptors can be seen (**asterisk**). Scale bars: 2 μm (**B**, **F**); 5 μm (**D**).

anemia,[10] fatty liver,[20] muscle weakness,[21] and hearing loss.[22,23] In addition to the AMD-like phenotypes,[11] we found a novel phenotype of the sensory retina of *Sod1*$^{-/-}$ mice. The slowly progressive degeneration of the retina appears to resemble the phenotype of the auditory system of *Sod1*$^{-/-}$ mice. Both the a- and b-waves of the ERGs were reduced in aged *Sod1*$^{-/-}$ mice. These results are compatible with the retinal histology showing the thinning of the INL and ONL. Because SOD1 is distributed throughout all retinal cell layers,[11] it is not surprising that SOD1 deficiency affected both the INL and ONL.

Recently, a relationship between oxidative stress and retinal degeneration has been reported in animal models. Antioxidants reduce the number of cone deaths in a model of retinitis pigmentosa,[24] and photo-oxidative stress causes retinal degeneration that can be rescued by antioxidants.[25] Our results provide additional evidence that antioxidants may be potentially protective for some types of age-related retinal degeneration. Administration of *N*-acetylcysteine (NAC) can rescue *Sod1*$^{-/-}$ mice against the effect of anemia by reversing the production of ROS in their erythrocytes.[10] It would be interesting to determine whether the retinal pathologies in *Sod1*$^{-/-}$ mice can be rescued by antioxidants including NAC, vitamins, or carotenoids. Our results showed no detectable differences in the apoptotic cell death between the retinas of *Sod1*$^{-/-}$ mice and the WT in the specimens examined. The nuclei of the retinal cells in senescent *Sod1*$^{-/-}$ mice were swollen suggesting that cell death may be caused by necrosis subsequent to elevated ROS attributable to the absence of SOD1.

Comparison with Other Models of Retinal Degeneration

Many animal models of retinal degeneration have been investigated.[3,4] Apoptosis is observed in some inherited retinal diseases such as retinitis pigmentosa and in other pathological retinal conditions such as hypoxia and oxidative stresses.[26,27] Several genetically mutated models of retinitis pigmentosa have been extensively investigated, including the RCS rat and *rd* mice. The retinal degeneration in the RCS rat is caused by an impairment of retinal pigmented epithelium because of mutation of receptor tyrosine kinase with subsequent photoreceptor cell death. The retinal cell death in RCS rat results from a caspase-1- and -2-dependent apoptosis.[7,27–30] *rd* mice have a recessive mutation of the gene encoding rod cGMP phosphodiesterase β-subunit, and photoreceptor apoptosis also occurs in a caspase-dependent manner.[6] A model of ROS-related retinal degeneration, mice deficient of *uchl3*, has been reported, and they show photoreceptor degeneration with TUNEL-positive cells, which begins at 2 to 3 weeks of age.[8]

These animal models of retinal degeneration differ from *Sod1*$^{-/-}$ mice; 1) *Sod1*$^{-/-}$ mice show very slow progressive degeneration, 2) the a- and b-waves are simultaneously affected, and 3) the death of the retinal cells appear to be caused mainly by necrosis rather than apoptosis. Because the *Sod2*$^{-/-}$ mice are not suitable for long-term follow-up studies,[17] *Sod1*$^{-/-}$ mice seem to be a good model to study ROS-mediated retinal degeneration. Recently, an intraocular injection of paraquat, a strong pro-oxidant, was reported to induce more severe retinal damage to the retina of *Sod1*$^{-/-}$ mice than that in the WT. This would indicate that SOD1 may be protective against excessive amounts of exogenous oxidative stress.[31] However, this study did not report the spontaneous retinal changes with age in *Sod1*$^{-/-}$ mice.

Relevance to Human Retinal Diseases

Oxidative stress is closely associated with retinal degeneration in humans.[32,33] Retinal degeneration is caused by ROS because of iron overload, ie, ocular siderosis.[32] Moreover, AMD is at present considered to be caused by elevated oxidative damages in retina because supple-

mentation by high-dose vitamins and minerals can slow the progression of AMD.[33] Patients with an early stage of AMD have decreased ERGs,[34–39] therefore, *Sod1*$^{-/-}$ mice may mimic the early retinal dysfunction attributable to aging. Excess light to the retina causes retinal degeneration by elevated production of ROS in retina. Therefore, we consider that our findings may help in the understanding of the pathophysiology of the ROS-mediated retinal degeneration in humans. Because nutritional intervention including vitamin A palmitate and ω-3-rich fish slow the progression of disease in many retinitis pigmentosa patients,[40] our findings support the hypothesis that antioxidants may be an additional interventional modality for some types of retinal degeneration.

In summary, we have demonstrated that SOD1 deficiency leads to retinal dysfunction and degenerative changes of retinal cell layers that are progressive. Because senescent *Sod1*$^{-/-}$ mice have choroidal neovascularization, a hallmark of wet-type AMD, *Sod1*$^{-/-}$ mice may exhibit features of both wet- and dry-type AMD. This implies that the etiology of these two clinically distinct entities in humans may be genetically identical.

Acknowledgments

We thank Satoshi Uchiyama, Ichie Kawamori, Yuka Kondo, and Chizuru Tsuda for technical assistance; Eiichiro Nagasaka and Masao Yoshikawa for ERG recording; Junko Moriya and Yumi Takanashi for histology; and Hisao Ohde for helpful discussion.

References

1. Valentine JS, Doucette PA, Potter SZ: Copper-zinc superoxide dismutase and amyotrophic lateral sclerosis. Annu Rev Biochem 2005, 74:563–593
2. Behndig A, Svensson B, Marklund SL, Karlsson K: Superoxide dismutase isoenzymes in the human eye. Invest Ophthalmol Vis Sci 1998, 39:471–475
3. Chang B, Hawes NL, Hurd RE, Davisson MT, Nusinowitz S, Heckenlively JR: Retinal degeneration mutants in the mouse. Vision Res 2002, 42:517–525
4. Dalke C, Graw J: Mouse mutants as models for congenital retinal disorders. Exp Eye Res 2005, 81:503–512
5. Grooten JV, Goossens B, Vanhaesebroeck B, Fiers W: Cell membrane permeabilization and cellular collapse, followed by loss of dehydrogenase activity: early events in tumor necrosis factor-induced cytotoxicity. Cytokine 1993, 5:546–555
6. Hopp RMP, Ransom N, Hilsenbeck SG, Papermaster DS, Windle JJ: Apoptosis in the murine rd1 retinal degeneration is predominantly p53-independent. Mol Vis 1998, 4:5
7. Katai N, Kikuchi T, Shibuki H, Kuroiwa S, Arai J, Kurokawa T, Yoshimura N: Caspase-like proteases activated in apoptotic photoreceptors of Royal College of Surgeons rats. Invest Ophthalmol Vis Sci 1999, 40:1802–1807
8. Sano Y, Furuta A, Setuie R, Kikuchi H, Wang YL, Sakurai M, Kwon J, Noda M, Wada K: Photoreceptor cell apoptosis in the retinal degeneration of Uchl3-deficient mice. Am J Pathol 2006, 169:132–141
9. Elchuri S, Oberley TD, Qi W, Eisenstein RS, Jackson Roberts L, Van Remmen H, Epstein CJ, Huang TT: CuZnSOD deficiency leads to persistent and widespread oxidative damage and hepatocarcinogenesis later in life. Oncogene 2005, 24:367–380
10. Iuchi Y, Okada F, Onuma K, Onoda T, Asano H, Kobayashi M, Fujii J: Elevated oxidative stress in erythrocytes due to a SOD1 deficiency causes anaemia and triggers autoantibody production. Biochem J 2007, 402:219–227
11. Imamura Y, Noda S, Hashizume K, Shinoda K, Yamaguchi M, Uchiyama S, Shimizu T, Mizushima Y, Shirasawa T, Tsubota K: Drusen, choroidal neovascularization, and retinal pigment epithelium dysfunction in SOD1-deficient mice: a model of age-related macular degeneration. Proc Natl Acad Sci USA 2006, 103:111282–111287
12. Goto Y, Peachey NS, Ripps H, Naash MI: Functional abnormalities in transgenic mice expressing a mutant rhodopsin gene. Invest Ophthalmol Vis Sci 1995,36:62–71
13. Sieving PA, Murayama K, Naarendrop F: Push-pull model of primate photopic electroretinogram: a role for hyperpolarizing neurons in shaping the b-wave. Vis Neurosci 1994, 11:519–532
14. Goto Y, Yasuda T, Tobimatsu S, Kato M: 20-Hz flicker stimulus can isolate the cone function in rat retina. Ophthalmic Res 1998, 30:368–373
15. Mori M, Metzqer D, Picaud S, Hindelang C, Simonutti M, Sahel J, Chambon P, Mark M: Retinal dystrophy resulting from ablation of RXR alpha in the mouse retinal pigment epithelium. Am J Pathol 2004, 164:701–710
16. Sandbach JM, Coscun PE, Grossniklaus HE, Kokoszka JE, Newman NJ, Wallace DC: Ocular pathology in mitochondrial superoxide dismutase (Sod2)-deficient mice. Invest Ophthalmol Vis Sci 2001, 42:2173–2178
17. Li Y, Huang TT, Carlson EJ, Melov S, Ursell PC, Olson JL, Noble LJ, Yoshimura MP, Berqer C, Chan PH, Wallace DC, Epstein CJ: Dilated cardiomyopathy and neonatal lethality in mutant mice lacking manganese superoxide dismutase. Nat Genet 1995, 11:376–381
18. Ikegami T, Suzuki Y, Shimizu T, Isono K, Koseki H, Shirasawa T: Model mice for tissue-specific deletion of the manganese superoxide dismutase (MnSOD) gene. Biochem Biophys Res Commun 2002, 296:729–736
19. Matzuk MM, Dionne L, Guo Q, Kumar TR, Lebovitz RM: Ovarian function in superoxide dismutase 1 and 2 knockout mice. Endocrinology 1998, 139:4008–4011
20. Uchiyama S, Shimizu T, Shirasawa T: CuZn-SOD deficiency causes ApoB degradation and induces hepatic lipid accumulation by impaired lipoprotein secretion in mice. J Biol Chem 2006, 281:31713–31719
21. Muller MF, Sonq W, Liu Y, Chaudhuri A, Pieke-Dahl S, Strong R, Huang TT, Epstein CJ, Roberts LJ II, Csete M, Faulkner JA, Van Remmen H: Absence of CuZn superoxide dismutase leads to elevated oxidative stress and acceleration of age-dependent skeletal muscle atrophy. Free Radic Biol Med 2006, 40:1993–2004
22. MacFadden SL, Ding D, Salvi R: Anatomical, metabolic and genetic aspects of age-related hearing loss in mice. Audiology 2001, 40:313–321
23. MacFadden SL, Ding D, Burkard RF, Jiang H, Reaume AG, Flood DG, Salvi RJ: Cu/Zn deficiency potentiates hearing loss and cochlear pathology in aged 129.CD-1 mice. J Comp Neurol 1999, 413:101–112
24. Komeima K, Roqers BS, Lu L, Campochiaro PA: Antioxidants reduce cone cell death in a model of retinitis pigmentosa. Proc Natl Acad Sci USA 2006, 103:11300–11305
25. Tanito M, Nishiyama A, Tanaka T, Masutani H, Nakamura H, Yodoi J, Ohira A: Change of redox status and modulation by thiol replenishment in retinal photooxidative damage. Invest Ophthalmol Vis Sci 2002, 43:2392–2400
26. Pacione LR, Szego MJ, Ikeda S, Nishina PM, McInnes RR: Progress toward understanding the genetic and biochemical mechanisms of inherited photoreceptor degenerations. Annu Rev Neurosci 2003, 26:657–700
27. Phelan JK, Bok D: A brief review of retinitis pigmentosa and the identified retinitis pigmentosa genes. Mol Vis 2000, 6:116–124
28. D'Cruz PM, Yasumura D, Weir J, Matthes MT, Abderrahim H, LaVail MM, Vollrath D: Mutation of the receptor tyrosine kinase gene Mertk in the retinal dystrophic RCS rat. Hum Mol Genet 2000, 9:645–651
29. Feng W, Yasumura D, Matthes MT, LaVail MM, Vollrath D: Mertk triggers uptake of photoreceptor outer segments during phagocytosis by cultured retinal pigment epithelial cells. J Biol Chem 2002, 277:17016–17022
30. Vollrath D, Feng W, Duncan JL, Yasumura D, D'Cruz PM, Chappelow A, Matthes MT, Kay MA, LaVail MM: Correction of the retinal dystrophy phenotype of the RCS rat by viral gene transfer of Mertk. Proc Natl Acad Sci USA 2001, 98:12584–12589
31. Dong A, Shen J, Krause M, Akiyama H, Hackett AF, Lai H, Campochiaro

PA: Superoxide dismutase 1 protects retinal cell from oxidative damage. J Cell Physiol 2006, 208:516–526
32. Weiss MJ, Hofeldt AJ, Behrens M, Fisher K: Ocular siderosis. Diagnosis and management. Retina 1997, 17:105–108
33. Age-Related Eye Disease Study Research Group: A randomized, placebo-controlled, clinical trial of high-dose supplementation with vitamins C and E and beta carotene for age-related cataract and vision loss: AREDS report no. 9. Arch Ophthalmol 2001, 119: 1439–1452
34. Hogg RE, Chakravarthy U: Visual function and dysfunction in early and late age-related maculopathy. Prog Ret Eye Res 2006, 25:249–276
35. Feigl B, Brown B, Lovie-Kitchin J, Swann P: The rod-mediated multifocal electroretinogram in aging and in early age-related maculopathy. Curr Eye Res 2006, 31:635–644
36. Gerth C, Delahunt PB, Alam S, Morse LS, Werner JS: Cone-mediated multifocal electoretinogram in age-related macular degeneration: progression over a long-term follow-up. Arch Ophthalmol 2006, 124:345–352
37. Jackson GR, McGwin G Jr, Phillips JM, Klein R, Owsley C: Impact of aging and age-related maculopathy on inactivation of the a-wave of the rod-mediated electroretinogram. Vision Res 2006, 46:1422–1431
38. Jackson GR, McGwin G Jr, Phillips JM, Klein R, Owsley C: Impact of aging and age-related maculopathy on inactivation of the a-wave of the rod-mediated electroretinogram. Invest Ophthalmol Vis Sci 2004, 45:3271–3278
39. Chen C, Wu L, Wu D, Huang S, Wen F, Luo G, Long S: The local cone and rod system function in early age-related macular degeneration. Doc Ophthalmol 2004, 109:1–8
40. Hartong DT, Berson EL, Dryja TP: Retinitis pigmentosa. Lancet 2006, 368:1795–1809